CRYSTALLOGRAPHIC COMMUNICATIONS

ISSN 2056-9890

Synthesis, crystal structure determination, Hirshfeld surface and crystal void analyses, interaction energy calculations and energy frameworks of *N*-(2-chlorophenyl)-*N*′-propanoylthiourea

Sharatha Kumar[a]* and Tuncer Hökelek[b]

[a]Department of Chemistry, Yenepoya Institute of Arts, Science, Commerce and Management, Mangaluru, Yenepoya University (Deemed to be university), 575013 Karnataka, India, and [b]Hacettepe University, Department of Physics, 06800 Beytepe-Ankara, Türkiye. *Correspondence e-mail: sharathyiascm@yenepoya.edu.in

Received 25 May 2026
Accepted 8 June 2026

Edited by B. Therrien, University of Neuchâtel, Switzerland

Keywords: propinoyl; thiourea; 2-chlorophenyl; crystal structure.

CCDC reference: 1816812

Supporting information: this article has supporting information at journals.iucr.org/e

The title compound, $C_{10}H_{11}ClN_2S$, consists of a chlorophenyl ring and a propanoyl moiety bridged over a thiourea functional group. The dihedral angle between the planar propinoyl and thiourea groups is 8.33 (14)°, and they are oriented at 48.50 (14) and 56.09 (6)° with respect to the phenyl ring. The intramolecular N—H···O hydrogen bond forms an S(6) ring motif. In the crystal, N—H···S hydrogen bonds link two molecules, enclosing $R_2^2(8)$ ring motifs, into centrosymmetric dimers. π–π stacking interactions help to consolidate the packing. Hirshfeld surface analysis revealed that the most important contributions for crystal packing are H···H (39.2%), H···Cl/Cl···H (15.8%), H···S/S···H (14.2%) and H···C/C···H (9.9%) interactions. The volume of the crystal voids and the percentage of free space were calculated to be 105.62 Å^3 and 9.33%, showing that there is no large cavity in the crystal packing. Computational methods indicated an N—H···S hydrogen-bonding energy of −53.5 kJ mol^{-1}. Evaluations of the electrostatic, dispersion and total energy frameworks indicate that the crystal cohesion is dominated by electrostatic energy contributions.

1. Chemical context

Thiourea is an important organic scaffold widely used in the development of therapeutic and industrially relevant molecules. Several applications have been reported, and researchers continue to explore thiourea derivatives in agriculture, gold recovery, analytical chemistry, and medicine (Rizki *et al.*, 2019; Shakeel *et al.*, 2016). Thiourea derivatives exhibit diverse biological activities, including anticancer (Nammalwar *et al.*, 2013), antithyroid, antimalarial (Mishra & Batra, 2013), antifungal, antiviral, antimicrobial, antioxidant, anti-allergic, anti-inflammatory, antiseptic, anti-leishmanial (Viana *et al.*, 2017), and anti-hypertensive effects.

The thiourea pharmacophore possesses unique chemical features, such as hydrogen-bonding groups (NH), a complementary sulfur site, and auxiliary binding positions at the 1,3-substituents, which enable strong and versatile interactions with biological targets (Mishra & Batra, 2013). Sulfur acts as a weak hydrogen-bond acceptor, while the bidentate nature of the thiourea protons enhances hydrogen bonding, making thiourea derivatives highly effective in medicinal chemistry (Nammalwar *et al.*, 2013).

We became interested in the properties and crystal structures of acylthioureas because of their notable biological activities, versatile metal-coordination behaviour, and ability to generate diverse supramolecular hydrogen-bonding

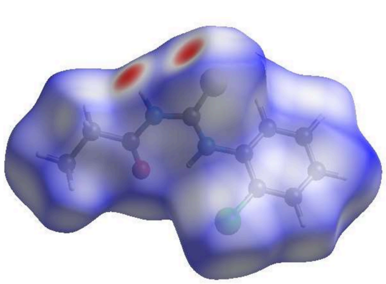

networks (Kumar *et al.*, 2012; Gowda *et al.*, 2012; Aly *et al.*, 2007; Saeed *et al.*, 2014, 2017). Numerous crystallographic investigations have demonstrated that acylthiourea derivatives adopt diverse conformations consolidated through intra- and intermolecular hydrogen bonding, particularly involving N—H···S and N—H···O interactions. These compounds also exhibit significant coordination versatility toward transition metals due to the presence of sulfur and carbonyl donor atoms. Detailed structural analyses of substituted acylthioureas have been reported in the literature (Arslan *et al.*, 2003; Ghosh *et al.*, 2010), highlighting the influence of the molecular geometry and supramolecular assembly on their physicochemical and biological properties.

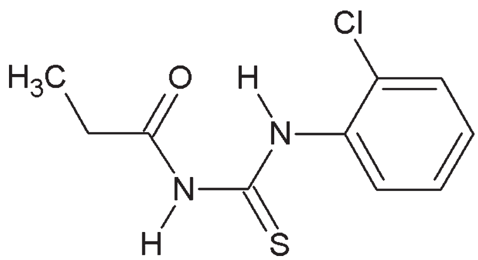

Herein, we report the molecular and crystal structures of *N*-(2-chlorophenyl)-*N*′-propanoylthiourea and Hirshfeld surface (HS) and crystal void analyses and interaction energy calculations and energy frameworks.

2. Structural commentary

The title compound consists of a chlorophenyl ring and propanoyl moiety bridged by a thiourea functional group (Fig. 1). The planar propinoyl (O1/C8–C10) and thiourea (S1/C7/N1/N2) groups (r.m.s. deviations of 0.039 and 0.013 Å, respectively) subtend a dihedral angle of 8.33 (14)°. The dihedral angles between the phenyl (C1–C6) ring and the propinoyl and thiourea groups are 48.50 (14) and 56.09 (6)°, respectively. The Cl1 and N1 atoms are 0.0037 (8) and −0.0345 (23) Å away from the best plane of the phenyl ring, so they are coplanar. The bond lengths are in normal ranges (Allen *et al.*, 1987) and comparable to those in the similar compounds *N*-(3-chloropropionyl)-*N*′-phenylthiourea (Othman *et al.*, 2010) and *N*-(2,6-dimethylphenyl)-*N*′ propanoylthiourea (Yusof *et al.*, 2012). The C1—N1—C7 [126.15 (19)°] and S1—C7—N1 [125.21 (18)°] bond angles are significantly wider, while the N1—C7—N2 [115.49 (19)°] and C2—C1—C6 [118.6 (2)°] are narrowed with respect to those found in these analogous structures. An intramolecular N—H···O hydrogen bond (Table 1) forms an *S*(6) ring motif (Etter *et al.*, 1990) (Fig. 2).

Table 1
Hydrogen-bond geometry (Å, °).

D—H···*A*	*D*—H	H···*A*	*D*···*A*	*D*—H···*A*
N1—H1*N*···O1	0.86 (2)	1.92 (2)	2.632 (3)	140 (3)
N2—H2*N*···S1^{i}	0.85 (2)	2.57 (2)	3.412 (2)	171 (3)

Symmetry code: (i) $-x, -y+2, -z$.

3. Supramolecular features

In the crystal, N—H···S hydrogen bonds (Table 1) link the molecules, enclosing $R_2^2(8)$ ring motifs (Etter *et al.*, 1990), into centrosymmetric dimers (Fig. 2). Weak π–π stacking interactions between parallel phenyl rings, with a centroid-to-centroid distance of 4.1188 (17) Å, help to consolidate the packing.

The intermolecular interactions in the crystal were visualized by carrying out the Hirshfeld surface (HS) analysis using *CrystalExplorer* 17.5 (Spackman *et al.*, 2021). Fig. 3 shows the Hirshfeld surface with several neighboring molecules in the crystal. The white surface indicates contacts with distances equal to the sum of van der Waals radii, and the red and blue colours indicate distances shorter (in close contact) or longer (distinct contacts) than the van der Waals radii, respectively. The red spots indicate their roles as the respective donors and/or acceptors atoms in hydrogen bonding, as discussed above. The π–π stacking interactions are shown in Fig. 4 by the presence of the adjacent red and blue triangles.

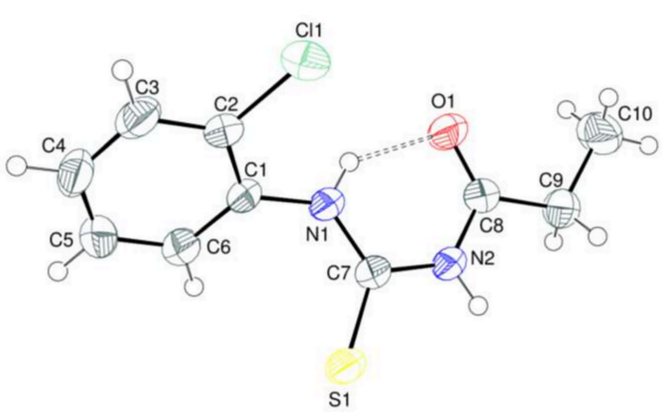

Figure 1
The asymmetric unit with atom-numbering scheme and 50% probability ellipsoids.

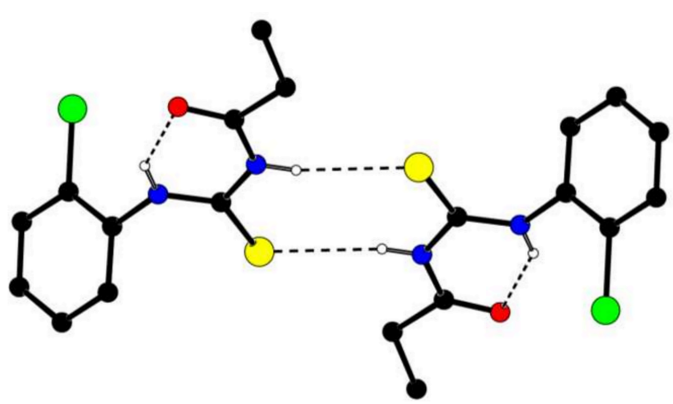

Figure 2
A partial packing diagram showing the intramolecular N—H···O and intermolecular N—H···S hydrogen bonds as dashed lines illustrating the intramolecular *S*(6) and intermolecular $R_2^2(8)$ ring motifs.

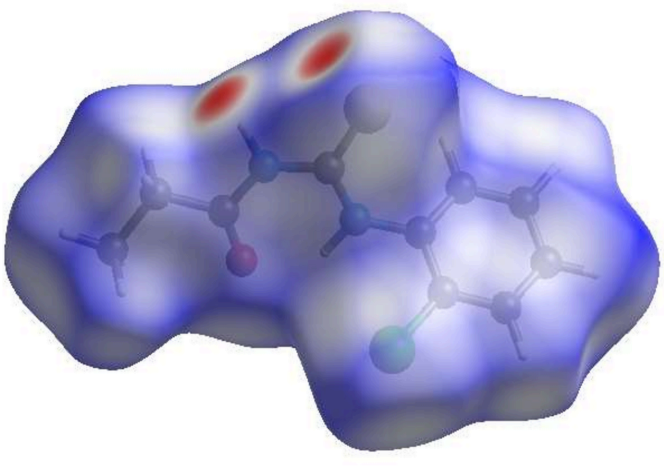

Figure 3
View of the three-dimensional Hirshfeld surface plotted over $d_{\rm norm}$ in the range −0.3374 to 1.1449 a.u.

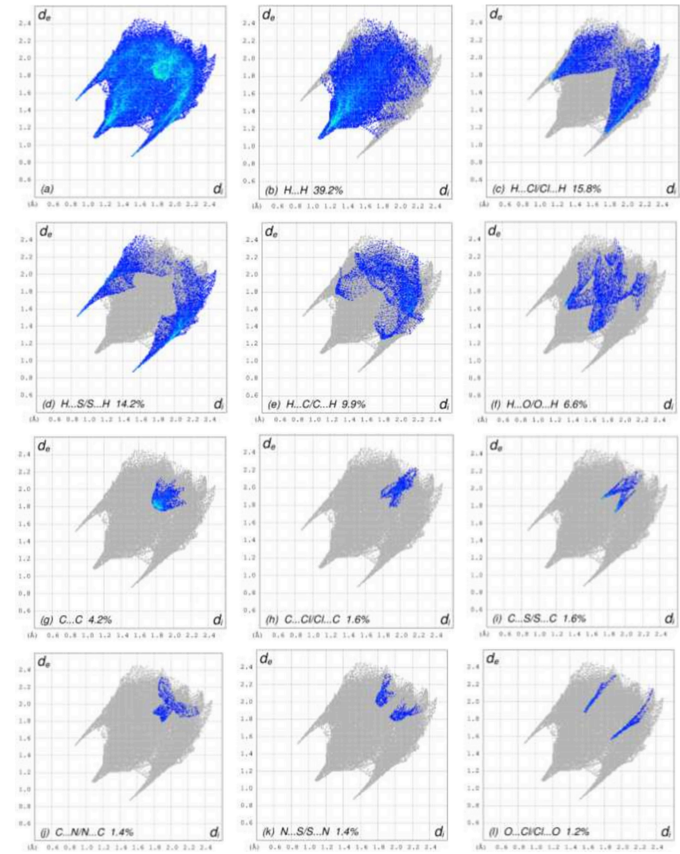

Figure 5
The full two-dimensional fingerprint plots for the title molecule, showing (*a*) all interactions, and delineated into (*b*) H···H, (*c*) H···Cl/Cl···H, (*d*) H···S/S···H, (*e*) H···C/C···H, (*f*) H···O/O···H, (*g*) C···C, (*h*) C···Cl/Cl···C, (i) C···S/S···C, (*j*) C···N/N···C, (*k*) N···S/S···N, (*l*) O···Cl/Cl···O, (*m*) H···N/N···H, (*n*) C···O/O···C, (*o*) N···O/O···N, (*p*) O···O and (*r*) S···S interactions. The $d_{\rm i}$ and $d_{\rm e}$ values are the closest internal and external distances (in Å) from given points on the Hirshfeld surface.

The overall two-dimensional fingerprint plot is shown in Fig. 5*a* and those delineated into H···H, H···Cl/Cl···H, H···S/S···H, H···C/C···H, H···O/O···H, C···C, C···Cl/Cl···C, S···C/C···S, N···C/C···N, N···S/S···N, O···Cl/Cl···O, H···N/N···H, O···O and S···S interactions are illustrated in Fig. 5*b*–*r*, respectively. According to the two-dimensional fingerprint plots, the H···H, H···Cl/Cl···H, H···S/S···H and H···C/C···H contacts make the most significant contributions to the HS, at 39.2%, 15.8%, 14.2% and 9.9%, respectively (Fig. 5).

The strength of the crystal packing depends on the tight packing of the molecules, which results insignificant voids. To check the strength of the crystal, a void analysis was performed. The volume of the crystal voids (Fig. 6*a*,*b*) and the percentage of free space in the unit cell were calculated as 105.62 Å^3 and 9.33%, respectively. Thus, the crystal packing appears compact.

The intermolecular interaction energies are calculated using CE–B3LYP/6–31G(d,p) energy model available in *CrystalExplorer17.5* (Spackman *et al.*, 2021), where a cluster of molecules is generated by applying crystallographic symmetry operations with respect to a selected central molecule within the radius of 3.8 Å by default. The total intermolecular energy ($E_{\rm tot}$) is the sum of electrostatic ($E_{\rm ele}$), polarization ($E_{\rm pol}$), dispersion ($E_{\rm dis}$) and exchange-repulsion ($E_{\rm rep}$) energies (Turner *et al.*, 2015) with scale factors of 1.057, 0.740, 0.871 and 0.618, respectively (Mackenzie *et al.*, 2017). The hydrogen-bonding interaction energies (in kJ mol^{-1}) for N2—H2*N*···S1 were calculated to be −70.5 ($E_{\rm ele}$), −12.5 ($E_{\rm pol}$), −19.9 ($E_{\rm dis}$), 77.0 ($E_{\rm rep}$) and −53.5 ($E_{\rm tot}$).

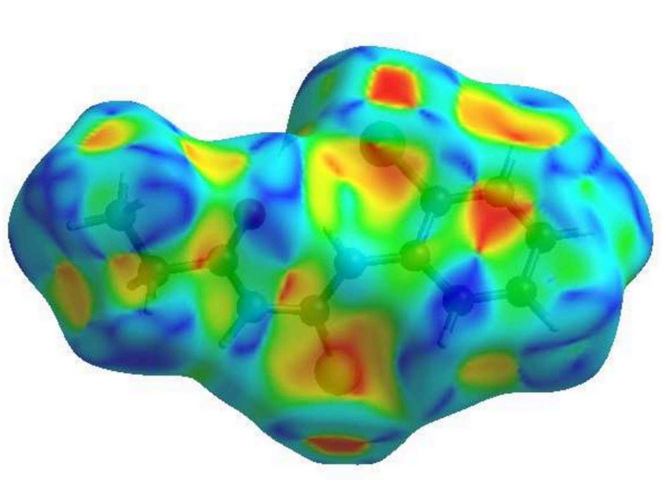

Figure 4
Hirshfeld surface plotted over shape-index showing the π–π interactions.

Energy frameworks combine the calculation of intermolecular interaction energies with a graphical representation of their magnitudes. They were constructed for $E_{\rm ele}$ (red cylinders), $E_{\rm dis}$ (green cylinders) and $E_{\rm tot}$ (blue cylinders) (Fig. 7*a*,*b*,*c*). Evaluation of the electrostatic, dispersion and total energy frameworks indicates that the stabilization of the crystal structure is dominated by the electrostatic energy contributions.

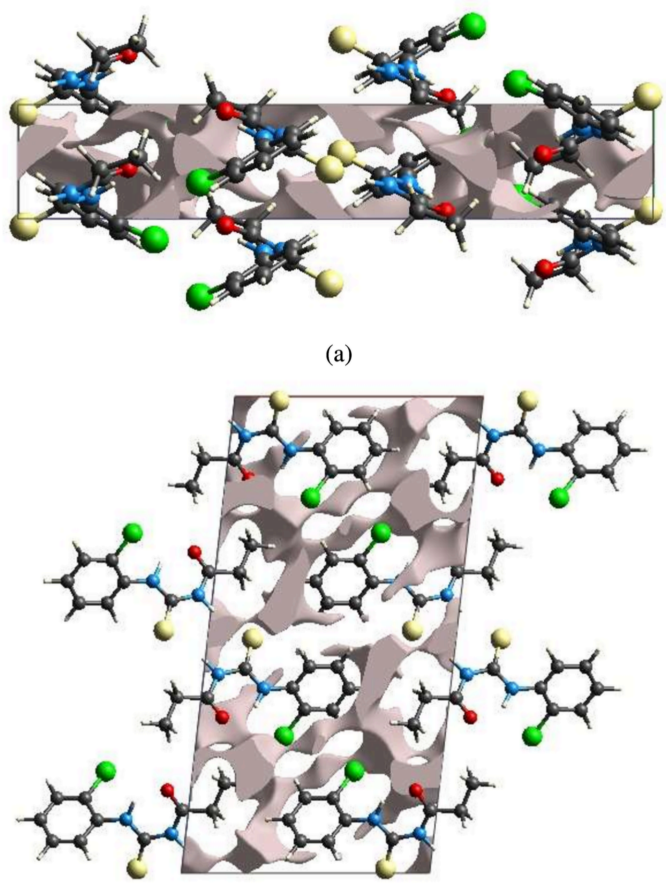

(a)

(b)

Figure 6
Crystal voids viewed down the (*a*) *a*-axis and (*b*) *b*-axis directions.

Table 2
Experimental details.

Crystal data	
Chemical formula	$C_{10}H_{11}ClN_2OS$
M_r	242.72
Crystal system, space group	Monoclinic, $P2_1/c$
Temperature (K)	293
a, b, c (Å)	11.971 (1), 4.1187 (6), 23.100 (2)
β (°)	96.44 (1)
V (Å^3)	1131.8 (2)
Z	4
Radiation type	Mo $K\alpha$
μ (mm^{-1})	0.50
Crystal size (mm)	0.50 × 0.48 × 0.36
Data collection	
Diffractometer	Oxford Diffraction Xcalibur with Sapphire CCD detector
Absorption correction	Multi-scan (*CrysAlis RED*; Oxford Diffraction, 2006)
T_{min}, T_{max}	0.790, 0.842
No. of measured, independent and observed [$I > 2\sigma(I)$] reflections	3971, 2291, 1809
R_{int}	0.012
$(\sin \theta/\lambda)_{max}$ (Å^{-1})	0.625
Refinement	
$R[F^2 > 2\sigma(F^2)]$, $wR(F^2)$, S	0.043, 0.113, 1.10
No. of reflections	2291
No. of parameters	143
No. of restraints	2
H-atom treatment	H atoms treated by a mixture of independent and constrained refinement
$\Delta\rho_{max}$, $\Delta\rho_{min}$ (e Å^{-3})	0.31, −0.25

Computer programs: *CrysAlis CCD* and *CrysAlis RED* (Oxford Diffraction, 2006), *SHELXT2014/5* (Sheldrick, 2015*a*), *SHELXL2018/3* (Sheldrick, 2015*b*), *ORTEP-3 for Windows* and *WinGX* publication routines (Farrugia, 2012) and *PLATON* (Spek, 2020).

4. Synthesis and crystallization

N-(2-Chlorophenyl)-*N*′-propanoylthiourea was synthesized by adding dropwise a solution of propinoyl chloride (0.10 mol) in acetone (30 ml) to a suspension of ammonium thiocyanate (0.10 mol) in acetone (30 ml), and then stirred for 2 h. The reaction mixture was then refluxed for 30 min. After cooling to room temperature, a solution of 2-chloroaniline (0.10 mol) in acetone (10 ml) was added and the solution refluxed for 3 h. After completion of the reaction (monitored by TLC), the reaction mixture was poured into acidified cold water. The precipitate was filtered under suction, washed with water and dried under vacuum. Colourless crystals suitable for X-ray analysis were obtained by slow evaporation of acetonitrile solution. White solid, yield 84%, m.p. 393–394 K. ^{1}H NMR (400 MHz, $CDCl_3$): δ (ppm) 12.30 (*s*, 1H), 9.77 (*s*, 1H), 7.23–7.61 (*m*, 4H, Ar-H), 1.45 (*t*, 3H, CH_3), 2.10 (*q*, 2H, CH_2). ^{13}C NMR (100 MHz, $CDCl_3$): δ (ppm) 24.4, 31.3, 124.0, 127.0, 128.0, 132.9, 137.4, 141.2, 171.0, 178.7.

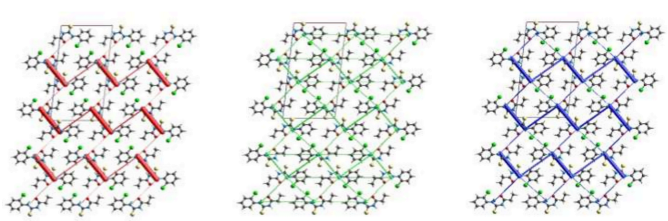

(a) (b) (c)

Figure 7
The energy frameworks for a cluster of molecules viewed down the *b*-axis showing the (*a*) electrostatic energy, (*b*) dispersion energy and (*c*) total energy diagrams. The cylindrical radius is proportional to the relative strength of the corresponding energies and they were adjusted to the same scale factor of 80 with cut-off value of 5 kJ mol^{-1} within 2 × 2 × 2 unit cells.

5. Refinement

Crystal data, data collection and structure refinement details are summarized in Table 2. The NH hydrogen atoms were located from difference-Fourier maps and refined isotropically. The C-bound H-atom positions were calculated geometrically at distances of 0.93 Å (for aromatic CH), 0.97 Å (for methylene CH) and 0.96 Å (for methyl CH) and refined using a riding model applying the constraint $U_{iso}(H) = k \times U_{eq}(C)$, where k = 1.5 for methyl hydrogens and 1.2 for the other H atoms.

Acknowledgements

The authors thank the Yenepoya Deemed to be University for the facilities and financial support. TH is also grateful to Hacettepe University Scientific Research Project Unit (grant No. 013 D04 602 004). The authors' contributions are as follows. Conceptualization, SK and TH; synthesis, SK; X-ray analysis, SK and TH; Hirshfeld surface analysis, TH; writing (review and editing of the manuscript) SK and TH; supervision, TH and SK.

References

Allen, F. H., Kennard, O., Watson, D. G., Brammer, L., Orpen, A. G. & Taylor, R. (1987). *J. Chem. Soc. Perkin Trans. 2* pp. S1–19.

Aly, A. A., Ahmed, E. K., El-Mokadem, K. M. & Hegazy, M. E. F. (2007). *J. Sulfur Chem.* **28**, 73–93.

Arslan, H., Flörke, U. & Külcü, N. (2003). *J. Chem. Crystallogr.* **33**, 919–924.

Etter, M. C., MacDonald, J. C. & Bernstein, J. (1990). *Acta Cryst.* B**46**, 256–262.

Farrugia, L. J. (2012). *J. Appl. Cryst.* **45**, 849–854.

Ghosh, H., Sarkar, S., Ali, A. R. & Patel, B. K. (2010). *J. Sulfur Chem.* **31**, 1–11.

Gowda, B. T., Foro, S. & Kumar, S. (2012). *Acta Cryst.* E**68**, o2338.

Kumar, S., Foro, S. & Gowda, B. T. (2012). *Acta Cryst.* E**68**, o2191.

Mackenzie, C. F., Spackman, P. R., Jayatilaka, D. & Spackman, M. A. (2017). *IUCrJ* **4**, 575–587.

Mishra, A. & Batra, S. (2013). *Curr. Top. Med. Chem.* **13**, 2011–2025.

Nammalwar, B., Berlin, K. D. & Bunce, R. A. (2013). *JSM Chem.* **1**, 1005.

Othman, E. A., Soh, S. K. C. & Yamin, B. M. (2010). *Acta Cryst.* E**66**, o628.

Oxford Diffraction (2006). *CrysAlis CCD* and *CrysAlis RED* Oxford Diffraction Ltd, Abingdon, England.

Rizki, I. N., Tanaka, Y. & Okibe, N. (2019). *Waste Manage. (Oxford)* **84**, 158–165.

Saeed, A., Flörke, U. & Erben, M. F. (2014). *J. Sulfur Chem.* **35**, 318–355.

Saeed, A., Qamar, R., Fattah, T. A., Flörke, U. & Erben, M. F. (2017). *Res. Chem. Intermed.* **43**, 3053–3093.

Shakeel, A., Altaf, A. A., Qureshi, A. M. & Badshah, A. (2016). *J. Drug Des. Med. Chem.* **2**, 10–20.

Sheldrick, G. M. (2015*a*). *Acta Cryst.* A**71**, 3–8.

Sheldrick, G. M. (2015*b*). *Acta Cryst.* C**71**, 3–8.

Spackman, P. R., Turner, M. J., McKinnon, J. J., Wolff, S. K., Grimwood, D. J., Jayatilaka, D. & Spackman, M. A. (2021). *J. Appl. Cryst.* **54**, 1006–1011.

Spek, A. L. (2020). *Acta Cryst.* E**76**, 1–11.

Turner, M. J., Thomas, S. P., Shi, M. W., Jayatilaka, D. & Spackman, M. A. (2015). *Chem. Commun.* **51**, 3735–3738.

Viana, G. M., Soares, D. C., Santana, M. V., do Amaral, L. H., Meireles, P. W., Nunes, R. P., da Silva, L. C. R. P., Aguiar, L. C. D., Rodrigues, C. R., de Sousa, V. P., Castro, H. C., Abreu, P. A., Sathler, P. C., Saraiva, E. M. & Cabral, L. M. (2017). *Chem. & Pharm. Bull.* **65**, 911–919.

Yusof, M. S. M., Mutalib, S. F. A., Arshad, S. & Razak, I. A. (2012). *Acta Cryst.* E**68**, o982.

supporting information

Acta Cryst. (2026). E**82**, 816-820 [https://doi.org/10.1107/S205698902600602X]

Synthesis, crystal structure determination, Hirshfeld surface and crystal void analyses, interaction energy calculations and energy frameworks of *N*-(2-chlorophenyl)-*N′*-propanoylthiourea

Sharatha Kumar and Tuncer Hökelek

Computing details

N-(2-Chlorophenyl)-*N′*-propanoylthiourea

Crystal data

$C_{10}H_{11}ClN_2OS$
M_r = 242.72
Monoclinic, $P2_1/c$
a = 11.971 (1) Å
b = 4.1187 (6) Å
c = 23.100 (2) Å
β = 96.44 (1)°
V = 1131.8 (2) Å^3
Z = 4
$F(000)$ = 504
D_x = 1.424 Mg m^{-3}
Mo $K\alpha$ radiation, λ = 0.71073 Å
Cell parameters from 2737 reflections
θ = 2.6–27.6°
μ = 0.50 mm^{-1}
T = 293 K
Prism, colorless
0.50 × 0.48 × 0.36 mm

Data collection

Oxford Diffraction Xcalibur with Sapphire CCD detector diffractometer
Rotation method data acquisition using ω scans.
Absorption correction: multi-scan (CrysAlis RED; Oxford Diffraction, 2006)
T_{min} = 0.790, T_{max} = 0.842
3971 measured reflections
2291 independent reflections
1809 reflections with $I > 2\sigma(I)$
R_{int} = 0.012
θ_{max} = 26.4°, θ_{min} = 2.6°
h = −14→11
k = −3→5
l = −21→28

Refinement

Refinement on F^2
Least-squares matrix: full
$R[F^2 > 2\sigma(F^2)]$ = 0.043
$wR(F^2)$ = 0.113
S = 1.10
2291 reflections
143 parameters
2 restraints
Hydrogen site location: mixed
H atoms treated by a mixture of independent and constrained refinement
$w = 1/[\sigma^2(F_o^2) + (0.0471P)^2 + 0.6068P]$ where $P = (F_o^2 + 2F_c^2)/3$
$(\Delta/\sigma)_{max}$ < 0.001
$\Delta\rho_{max}$ = 0.31 e Å^{-3}
$\Delta\rho_{min}$ = −0.25 e Å^{-3}

Special details

Geometry. All esds (except the esd in the dihedral angle between two l.s. planes) are estimated using the full covariance matrix. The cell esds are taken into account individually in the estimation of esds in distances, angles and torsion angles; correlations between esds in cell parameters are only used when they are defined by crystal symmetry. An approximate (isotropic) treatment of cell esds is used for estimating esds involving l.s. planes.

Fractional atomic coordinates and isotropic or equivalent isotropic displacement parameters (Å²)

	x	y	z	U_{iso}*/U_{eq}
Cl1	0.35101 (6)	1.1838 (2)	0.21334 (3)	0.0615 (2)
S1	0.18007 (5)	1.06937 (19)	0.00913 (3)	0.0500 (2)
O1	0.09369 (15)	0.5612 (6)	0.17325 (7)	0.0683 (6)
N1	0.24754 (16)	0.8040 (6)	0.11267 (8)	0.0434 (5)
N2	0.05779 (16)	0.7857 (6)	0.08305 (8)	0.0414 (5)
C1	0.36338 (18)	0.8729 (6)	0.11114 (9)	0.0381 (5)
C2	0.4218 (2)	1.0438 (6)	0.15665 (9)	0.0402 (6)
C3	0.5355 (2)	1.1061 (7)	0.15738 (11)	0.0516 (7)
H3	0.573956	1.219918	0.188205	0.062*
C4	0.5911 (2)	0.9986 (7)	0.11229 (11)	0.0548 (7)
H4	0.667268	1.042699	0.112239	0.066*
C5	0.5347 (2)	0.8257 (7)	0.06703 (11)	0.0540 (7)
H5	0.572970	0.751932	0.036720	0.065*
C6	0.4216 (2)	0.7618 (7)	0.06657 (10)	0.0466 (6)
H6	0.384135	0.643217	0.036089	0.056*
C7	0.16460 (19)	0.8754 (6)	0.07130 (9)	0.0375 (5)
C8	0.02653 (19)	0.6352 (7)	0.13210 (10)	0.0435 (6)
C9	−0.0974 (2)	0.5694 (7)	0.13048 (10)	0.0487 (6)
H9A	−0.118402	0.402049	0.101768	0.058*
H9B	−0.138509	0.764965	0.118118	0.058*
C10	−0.1317 (2)	0.4623 (9)	0.18860 (12)	0.0687 (9)
H10A	−0.111548	0.627255	0.217244	0.103*
H10B	−0.093709	0.263737	0.200384	0.103*
H10C	−0.211450	0.427960	0.185048	0.103*
H1N	0.227 (3)	0.712 (7)	0.1431 (10)	0.082*
H2N	0.004 (2)	0.821 (8)	0.0569 (11)	0.082*

Atomic displacement parameters (Å²)

	U^{11}	U^{22}	U^{33}	U^{12}	U^{13}	U^{23}
Cl1	0.0633 (5)	0.0837 (6)	0.0373 (3)	0.0074 (4)	0.0045 (3)	−0.0067 (3)
S1	0.0348 (3)	0.0719 (5)	0.0415 (3)	−0.0044 (3)	−0.0031 (2)	0.0171 (3)
O1	0.0401 (10)	0.1185 (19)	0.0455 (10)	0.0024 (11)	0.0009 (8)	0.0306 (11)
N1	0.0303 (10)	0.0661 (15)	0.0327 (10)	−0.0021 (10)	−0.0020 (8)	0.0078 (10)
N2	0.0293 (10)	0.0591 (13)	0.0348 (10)	0.0000 (10)	−0.0015 (7)	0.0061 (9)
C1	0.0301 (11)	0.0487 (15)	0.0343 (11)	0.0039 (10)	−0.0015 (9)	0.0078 (10)
C2	0.0384 (13)	0.0499 (15)	0.0312 (11)	0.0041 (11)	−0.0015 (9)	0.0059 (10)
C3	0.0421 (14)	0.0605 (18)	0.0487 (14)	−0.0061 (13)	−0.0105 (11)	0.0023 (13)
C4	0.0298 (13)	0.070 (2)	0.0634 (17)	−0.0012 (13)	0.0018 (11)	0.0100 (15)

C5	0.0426 (14)	0.0710 (19)	0.0498 (14)	0.0126 (14)	0.0112 (11)	0.0060 (14)
C6	0.0400 (13)	0.0608 (17)	0.0382 (12)	0.0042 (12)	0.0004 (10)	−0.0028 (12)
C7	0.0340 (12)	0.0453 (14)	0.0322 (11)	0.0009 (10)	−0.0013 (9)	−0.0009 (10)
C8	0.0382 (13)	0.0564 (17)	0.0356 (12)	0.0023 (12)	0.0032 (10)	0.0035 (11)
C9	0.0368 (13)	0.0617 (17)	0.0474 (13)	−0.0064 (13)	0.0039 (10)	0.0025 (13)
C10	0.0550 (17)	0.099 (3)	0.0533 (16)	−0.0196 (18)	0.0133 (13)	0.0054 (17)

Geometric parameters (Å, º)

Cl1—C2	1.736 (2)	C3—H3	0.9300
S1—C7	1.672 (2)	C4—C5	1.378 (4)
O1—C8	1.213 (3)	C4—H4	0.9300
N1—C7	1.331 (3)	C5—C6	1.377 (3)
N1—C1	1.420 (3)	C5—H5	0.9300
N1—H1N	0.858 (17)	C6—H6	0.9300
N2—C8	1.380 (3)	C8—C9	1.504 (3)
N2—C7	1.387 (3)	C9—C10	1.513 (3)
N2—H2N	0.847 (17)	C9—H9A	0.9700
C1—C6	1.384 (3)	C9—H9B	0.9700
C1—C2	1.387 (3)	C10—H10A	0.9600
C2—C3	1.384 (3)	C10—H10B	0.9600
C3—C4	1.371 (4)	C10—H10C	0.9600
C7—N1—C1	126.15 (19)	C5—C6—C1	120.5 (2)
C7—N1—H1N	115 (2)	C5—C6—H6	119.8
C1—N1—H1N	118 (2)	C1—C6—H6	119.8
C8—N2—C7	128.42 (19)	N1—C7—N2	115.49 (19)
C8—N2—H2N	114 (2)	N1—C7—S1	125.21 (18)
C7—N2—H2N	118 (2)	N2—C7—S1	119.27 (16)
C6—C1—C2	118.6 (2)	O1—C8—N2	122.6 (2)
C6—C1—N1	121.8 (2)	O1—C8—C9	122.6 (2)
C2—C1—N1	119.6 (2)	N2—C8—C9	114.7 (2)
C3—C2—C1	121.0 (2)	C8—C9—C10	113.3 (2)
C3—C2—Cl1	119.47 (19)	C8—C9—H9A	108.9
C1—C2—Cl1	119.52 (18)	C10—C9—H9A	108.9
C4—C3—C2	119.4 (2)	C8—C9—H9B	108.9
C4—C3—H3	120.3	C10—C9—H9B	108.9
C2—C3—H3	120.3	H9A—C9—H9B	107.7
C3—C4—C5	120.3 (2)	C9—C10—H10A	109.5
C3—C4—H4	119.8	C9—C10—H10B	109.5
C5—C4—H4	119.8	H10A—C10—H10B	109.5
C6—C5—C4	120.1 (2)	C9—C10—H10C	109.5
C6—C5—H5	119.9	H10A—C10—H10C	109.5
C4—C5—H5	119.9	H10B—C10—H10C	109.5
C7—N1—C1—C6	−56.9 (4)	C2—C1—C6—C5	−1.2 (4)
C7—N1—C1—C2	126.0 (3)	N1—C1—C6—C5	−178.4 (2)
C6—C1—C2—C3	0.8 (4)	C1—N1—C7—N2	−179.4 (2)

N1—C1—C2—C3	178.0 (2)	C1—N1—C7—S1	−1.3 (4)
C6—C1—C2—Cl1	−179.63 (19)	C8—N2—C7—N1	0.6 (4)
N1—C1—C2—Cl1	−2.4 (3)	C8—N2—C7—S1	−177.7 (2)
C1—C2—C3—C4	0.3 (4)	C7—N2—C8—O1	0.4 (5)
Cl1—C2—C3—C4	−179.3 (2)	C7—N2—C8—C9	−179.5 (2)
C2—C3—C4—C5	−1.0 (4)	O1—C8—C9—C10	10.7 (4)
C3—C4—C5—C6	0.5 (4)	N2—C8—C9—C10	−169.4 (3)
C4—C5—C6—C1	0.6 (4)		

Hydrogen-bond geometry (Å, º)

D—H···*A*	*D*—H	H···*A*	*D*···*A*	*D*—H···*A*
N1—H1*N*···O1	0.86 (2)	1.92 (2)	2.632 (3)	140 (3)
N2—H2*N*···S1^{i}	0.85 (2)	2.57 (2)	3.412 (2)	171 (3)

Symmetry code: (i) $-x, -y+2, -z$.